JOURNAL OF MATERIALS SCIENCE **34** (1999) 2495–2505

Synthesis of silicon carbide foams from polymeric precursors and their blends

X. BAO, M. R. NANGREJO, M. J. EDIRISINGHE
Institute of Polymer Technology & Materials Engineering, Loughborough University, Loughborough, Leicestershire LE11 3TU, UK
E-mail: m.j.edirisinghe@lboro.ac.uk

Several polysilanes with different overall functionalities have been synthesized and pyrolyzed to produce porous silicon carbide. The polysilanes and their ceramic products have been characterized using gel permeation chromatography, Fourier transform-infrared spectroscopy, thermogravimetry, X-ray diffractometry and microscopy. Some products were foams while others were micro-porous ceramics. The effect of the final pyrolytic yield on the type of ceramic produced, its pore structure and shape retention are discussed. Two polysilanes were blended in various ratios to control the pyrolysis process more precisely. This allowed the type, shape and pore-structure of the silicon carbide produced to be controlled more efficiently. There exists a relationship between the composition and structure of the precursors and their final pyrolytic yield and this determines the type, shape retainability and pore structure of the ceramics produced. In this work, precursors or their blends which gave a final pyrolytic yield of 50–60 wt % produced the best silicon carbide foams.

1. Introduction

There is considerable interest in engineering ceramic foams which possess a number of favourable properties such as low density, low thermal conductivity, thermal stability, high specific strength and high resistance to chemical attack and are suitable for industrial applications such as high temperature thermal insulation, hot gas particulate filters, hot metal filters, catalyst supports and cores in high temperature structural panels [1–3].

Ceramic foams can be produced by different methods such as impregnation of polymer foams with slurries containing appropriate binders and ceramic particles followed by pressureless sintering at elevated temperatures [4, 5], chemical vapour deposition of ceramics on to a porous carbon skeleton [6], sol-gel processes that develop porosity during phase transformations and chemical reactions [7], siliciding carbon foams [8], a gel-cast foam process which combines the foaming of ceramic suspensions and *in-situ* polymerization [9] and a replication process where polymer is injected into a porous substrate, such as sodium chloride which is removed later to produce carbon and silicon carbide (SiC) foams [10–12]. Ceramic foams obtained through a co-blowing mechanism from a mixture of polycarbosilane and polyurethane have also been reported [13].

In the research described in this paper, ceramic foam was synthesized directly from polymeric precursors. As an example, SiC foams were prepared in this manner from polysilanes and their blends. The use of polymeric precursors to produce ceramics offers distinct advantages over traditional ceramic forming methods, mainly the use of polymer processing techniques at relatively low temperatures [e.g. 14–19]. However, at present this processing method is largely limited to the preparation of ceramic fibres rather than dense ceramic products because a high porosity is experienced during the conversion of the polymer to the ceramic due to the release of various elements from the polymer in the form of low molecular weight gases [15, 20]. Nevertheless, this limitation could be circumvented if the polymeric precursors are pyrolyzed to produce ceramic foams. Moreover, as the ceramic foam is formed due to volatiles generated by the decomposition of the polymeric precursors during pyrolysis, it is possible to control the porosity of the ceramics by controlling the gas evaporation by tailoring the composition and structure of the polymers. Hence, a series of polysilanes with different substituents were synthesized, blended and used as precursors for the synthesis of SiC foams. The precursors and their blends were pyrolyzed in an inert atmosphere and some formulations produced ceramic foams. The relationship between the structures of the polymeric precursors and their ability to produce ceramic foams are discussed with the aid of infrared spectroscopy, thermogravimetry and microscopy studies.

2. Experimental

2.1. Synthesis of polysilanes

The polysilanes discussed in this paper were synthesized by the alkali dechlorination of various combinations of chlorinated silane monomers in refluxing toluene/tetrahydrofuran with molten sodium as

TABLE I Monomers used in the synthesis of polysilanes, f refers to functionality

Monomers	Formula	f	Abbreviations
Dichloro-methylphenylsilane	$(CH_3)(C_6H_5)SiCl_2$	2	MP
Dichloromethylsilane	$(CH_3)HSiCl_2$	3	MH
Dichlorophenylsilane	$(C_6H_5)HSiCl_2$	3	PH
Trichloromethylsilane	CH_3SiCl_3	3	TCM
Trichlorophenylsilane	$C_6H_5SiCl_3$	3	TCP
Dichloro-methylvinylsilane	$(CH_3)(CH_2{=}CH)SiCl_2$	4	MVin

described previously [21–23]. Details of the various monomers used are summarized in Table I.

2.2. Preparation of polymer blends

A boron carbide mortar and pestle was used to mix various proportions of polymeric precursors (P2 and P9) in order to prepare blends containing 20, 40, 60 and 80 wt % of PS2.

2.3. Pyrolysis and crystallization

Pressed pellets (∼8 mm diameter and ∼3 mm thick) of the polymeric precursors and their blends were placed in an alumina boat and heated from the ambient temperature to 900 °C at 2 °C min^{-1} in a tube furnace (Lenton Thermal Designs Ltd., Harborough, UK) in the presence of flowing nitrogen (flow rate approximately 250 ml min^{-1}) followed by soaking at this temperature for 2 hours. Subsequently, the furnace was switched off and allowed to cool to the ambient temperature. Crystallization was carried out by heating the pyrolyzed residue in a tube furnace in the presence of flowing nitrogen (flow rate approximately 250 ml min^{-1}) from the ambient temperature to different final temperatures (1100 to 1700 °C) at 2 °C min^{-1} followed by soaking at this temperature for 2 hours and, then, cooling to the ambient temperature at 2 °C min^{-1}.

2.4. Characterization

The molecular weights of the polysilanes were determined by gel permeation chromatography (GPC) carried out at RAPRA Technology Ltd., Shrewsbury, UK. GPC studies were calibrated using polystyrene standards and with chloroform as the eluent. The flow rate used was 1.0 ml/min. Fourier transform-infrared (FT-IR) spectra of as-synthesized polymer samples were obtained using a Nicolet 710 spectrometer. 1 mg of each polymer was ground and mixed with 150 mg of dried KBr powder and pressed into a pellet. Spectra were obtained in the range of 4000–400 cm^{-1} with a resolution of 4 cm^{-1}.

The pyrolytic yield from each polymer was measured by thermogravimetry. Samples were heated from the ambient temperature up to 900 °C in flowing nitrogen

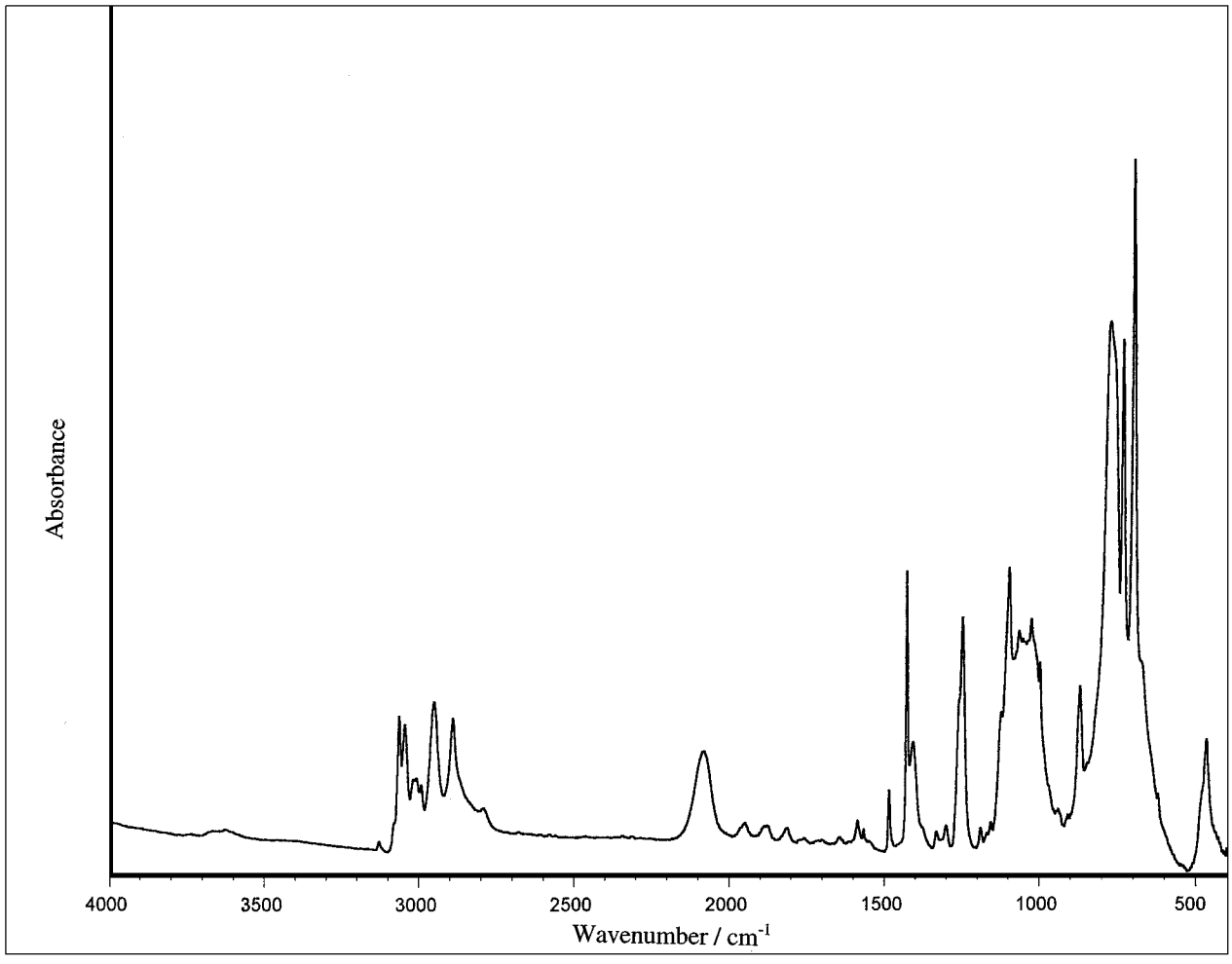

Figure 1 FT-IR spectrum of polysilane P5.

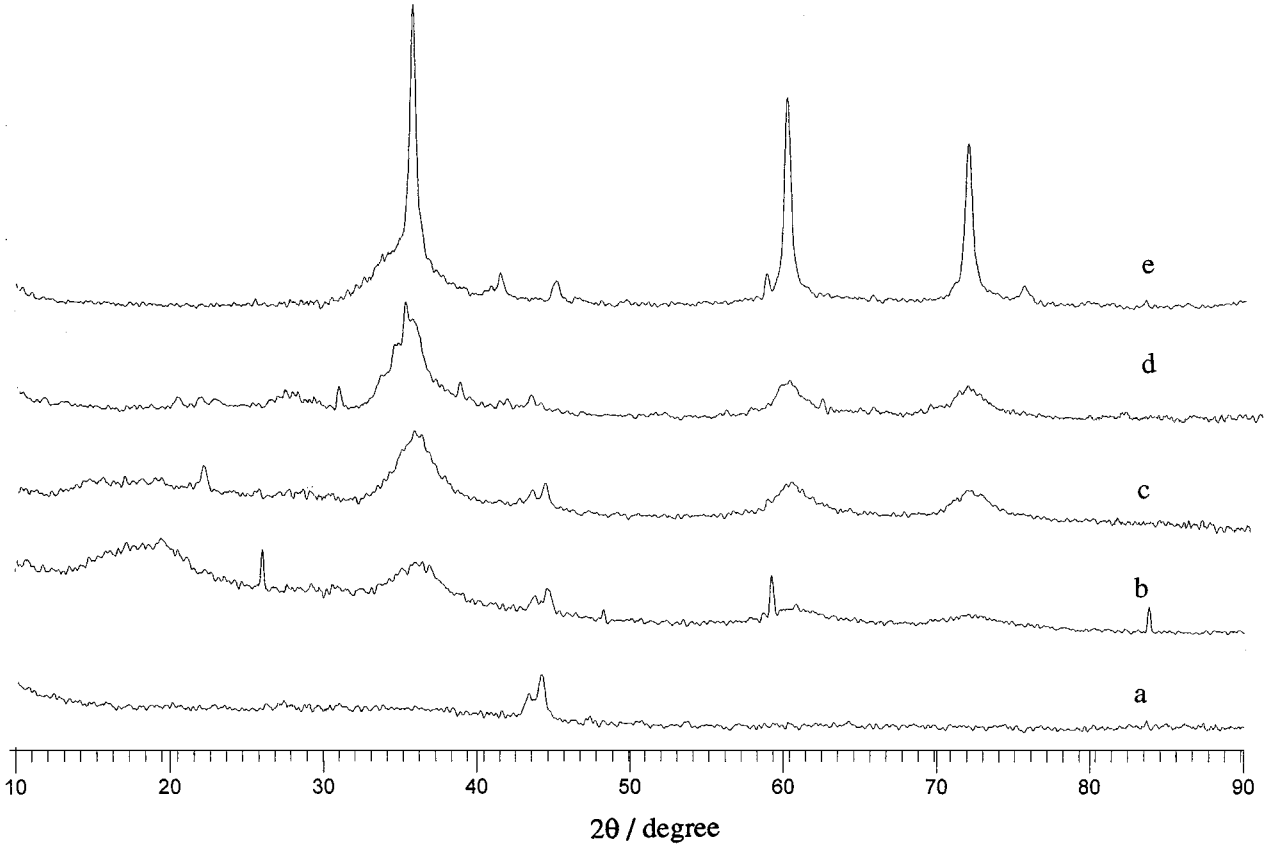

Figure 2 XRD patterns of ceramics derived from polysilane P5 after pyrolyzing and crystallizing at (a) 1100 °C, (b) 1300 °C, (c) 1500 °C, (d) 1600 °C and (e) 1700 °C.

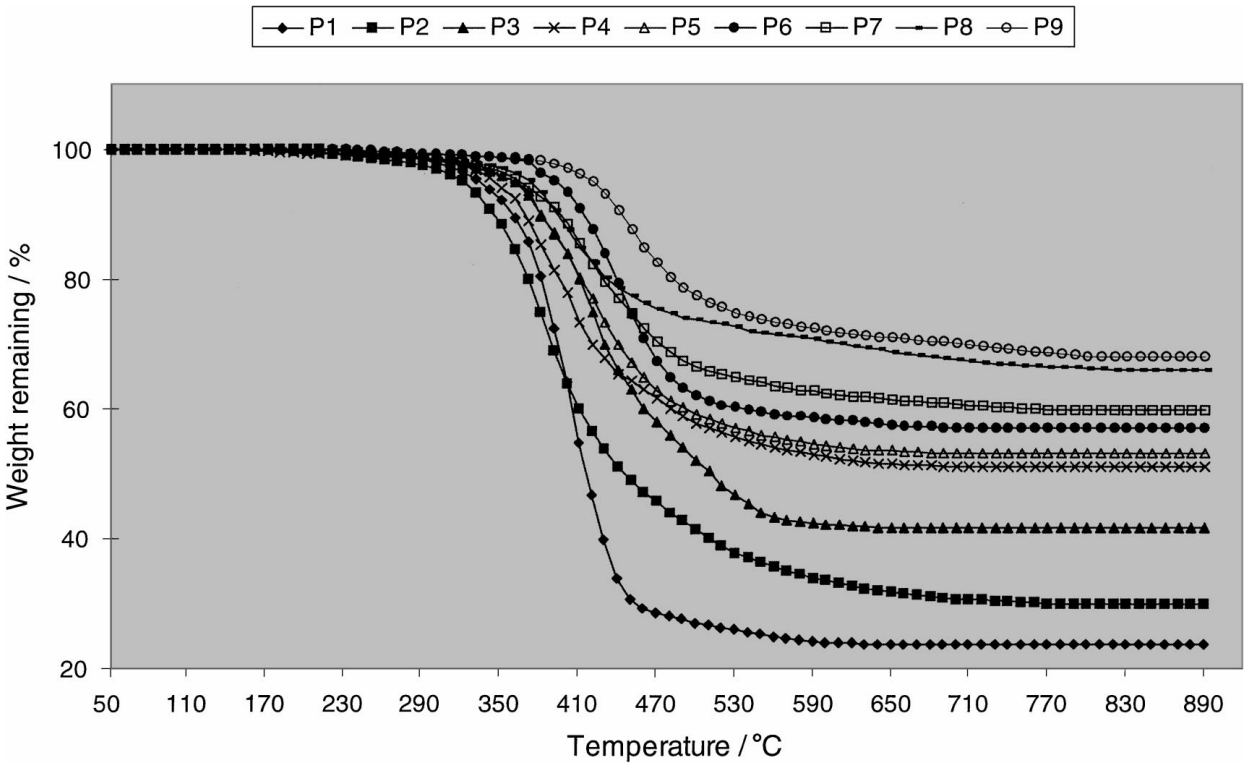

Figure 3 Thermogravimetric traces of polymeric precursors P1–P9.

(0.5 ml min^{-1}) at 10 °C min^{-1} in a Perkin-Elmer TGA 7 to determine the pyrolytic yield.

The macro-appearance of the discs after pyrolysis was photographed. The microstructures of the cross-sections of the pyrolyzed products were investigated using a Stereogun 360 scanning electron microscope (SEM). Samples studied using the SEM were coated with gold.

X-ray diffraction (XRD) was carried out on the polysilanes after pyrolysis to various final temperatures

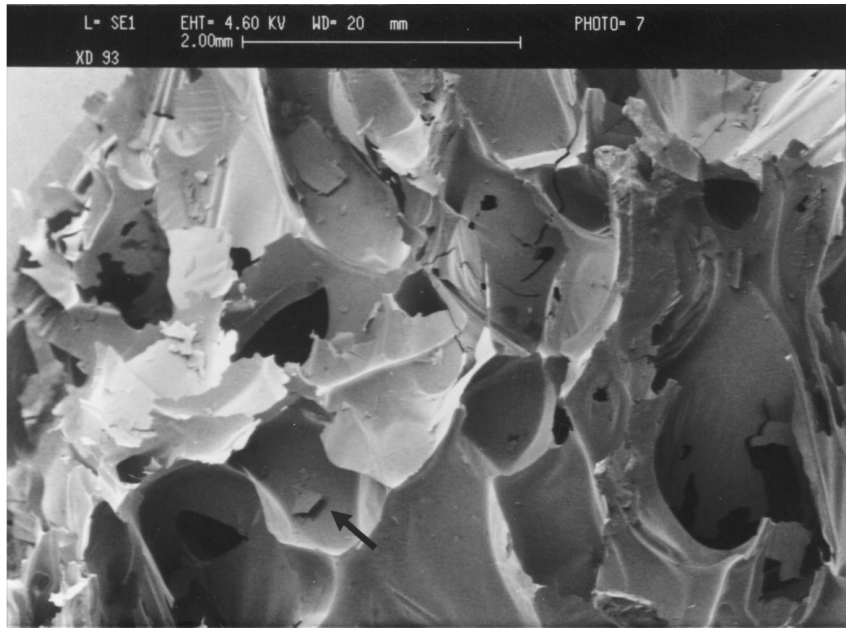

(a)

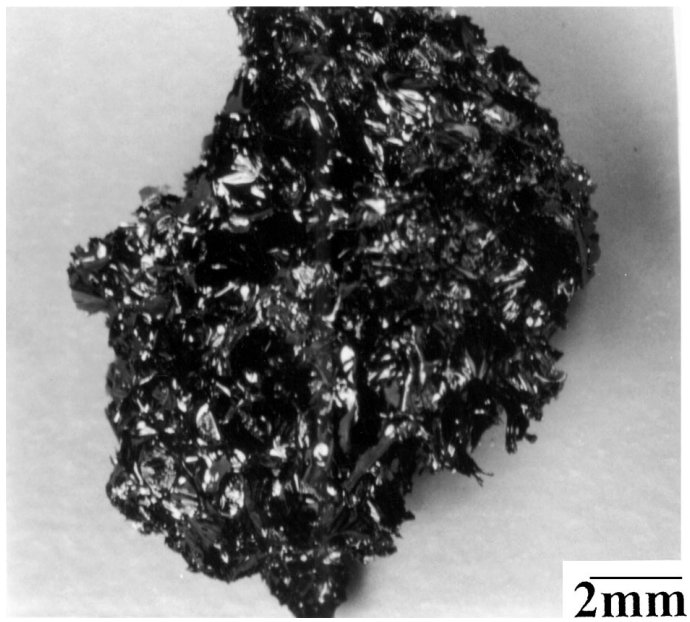

(b)

Figure 4 (a) Scanning electron micrograph of cross-section and (b) macro-appearance of pyrolyzed polymeric precursor P2. A pore covered by a membrane is indicated by an arrow in Fig. 4a.

($\geq$1100 °C) in nitrogen. Samples for X-ray diffractometry were ground using a boron carbide mortar and pestle. A small amount of industrial methylated spirit (IMS) was added during grinding and the paste produced was placed on a single silicon plate. The IMS was allowed to evaporate before XRD analysis was conducted. A Philips X-ray diffractometer was used with the silicon plate attached to a 20 mm diameter stainless steel stub. Ni filtered Cu$K\alpha$ radiation of wavelength 0.15406 nm was used. The voltage and current settings of the diffractometer were 35 kV and 20 mA, respectively. The scan range was from 10° to 90° with a step size of 0.021° and a scan speed of 0.02° s^{-1}.

3. Results and discussion

3.1. Polymer synthesis and characterization

Polysilanes were prepared with different starting monomers of different functionality (f), as shown in Table I. The proportion of each was altered to give different values of the overall functionality, F, as defined by Equation 1.

$$F = \frac{x f_1 + y f_2 + z f_3}{x + y + z} \quad (1)$$

where f_1, f_2 and f_3 are the respective molar functionalities of the monomers reacted in the molar ratio $x : y : z$.

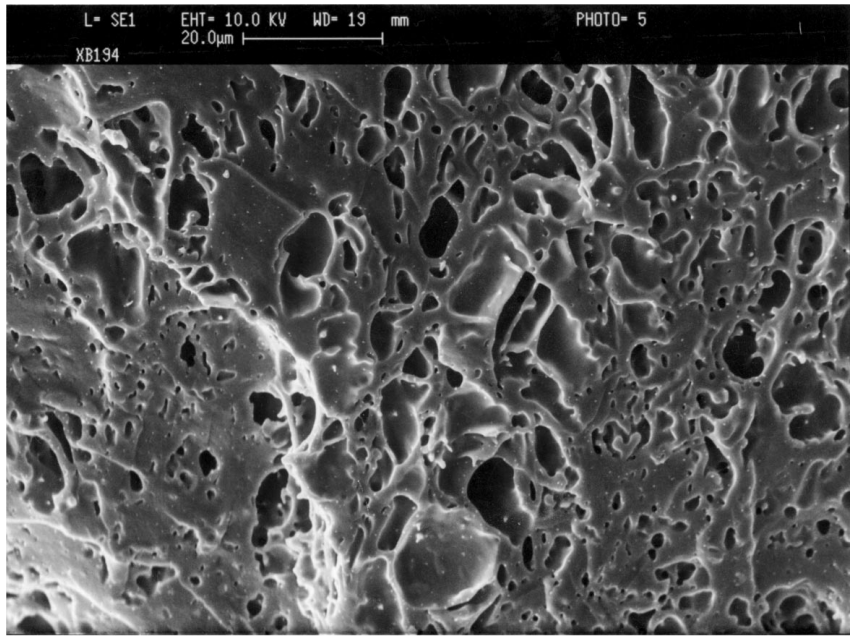

(a)

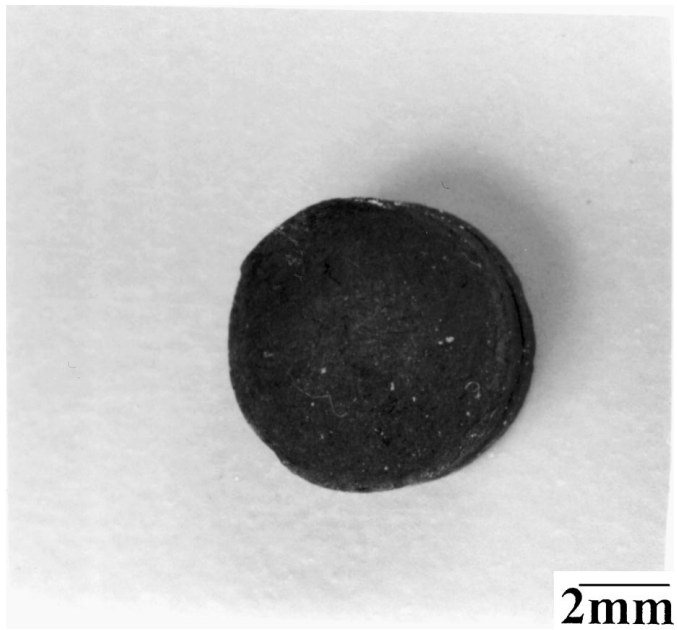

(b)

Figure 5 (a) Scanning electron micrograph of cross-section and (b) macro-appearance of pyrolyzed polymeric precursor P9.

Each reaction leads to the production of three different polymer fractions, i.e. insoluble solid (IS), soluble solid (SS) and soluble liquid (SL). Both SS and SL fractions are soluble in toluene and tetrahydrofuran at room temperature. The SS fraction is used as the ceramic precursor and the yields obtained are given in Table II. The calculated values of $\bar{M}_n$, $\bar{M}_w$, and the polydispersity $\bar{M}_w/\bar{M}_n$, which is a measure of the width of the molecular weight distribution, for all the samples discussed in the present work are also given in Table II.

As an example, a typical FT-IR spectrum of a terpolysilane (P5) is shown in Fig. 1. It exhibits characteristic C-H stretching between 3100 and 2700 cm^{-1}. The peaks at 3050 and 3067 cm^{-1} represent C-H stretching in the phenyl group. Methyl group stretching is observed at 2956 and 2894 cm^{-1}. Additional peaks at 1406 and 1248 cm^{-1} are characteristic of the asymmetric and symmetric bending modes, respectively, of CH_3 bonded to silicon. Three small peaks at 1949, 1887 and 1815 cm^{-1} are attributed to the phenyl-Si vibration. The peaks at low wavenumbers of 697 cm^{-1} for Si-C stretching and 464 cm^{-1} for Si-Si are typical [24–26]. Two characteristic peaks at 1589 and 2081 cm^{-1}, where the vinyl group and the Si-H group occurs, are clearly present [27–29]. FT-IR spectra of similar co- and terpolysilanes are discussed in more detail in our previous work [21, 22].

TABLE II Details of monomer(s) used in the synthesis, overall functionality (F), polymer yield, molecular weight and pyrolytic yield of each polymer

Polymer	Monomer(s) used (mol %)	F	Polymer yield (wt %)	$\bar{M}_w$	$\bar{M}_n$	$\bar{M}_w/\bar{M}_n$	Pyrolytic yield (wt %)
P1	MP = 100	2.0	43	7680	1520	5.1	23.6
P2	MP/TCM = 70/30	2.3	60	4270	1840	2.3	30.4
P3	MP/MVin = 70/30	2.6	37	6970	1670	4.2	42.1
P4	MP/MVin/TCM = 60/20/20	2.6	28	3570	1560	2.3	51.0
P5	MP/MVin/MH = 60/20/20	2.6	38	12000	2460	4.9	53.2
P6	MP/MVin/TCM = 55/15/30	2.6	52	4240	1510	2.8	56.8
P7	MP/MVin/TCM = 55/30/15	2.75	45	5240	1600	3.3	59.8
P8	PH/MVin/TCP = 60/20/20	3.2	70	7700	1580	4.9	66.4
P9	PH/MVin/TCM = 60/20/20	3.2	32	8700	2580	3.4	67.9

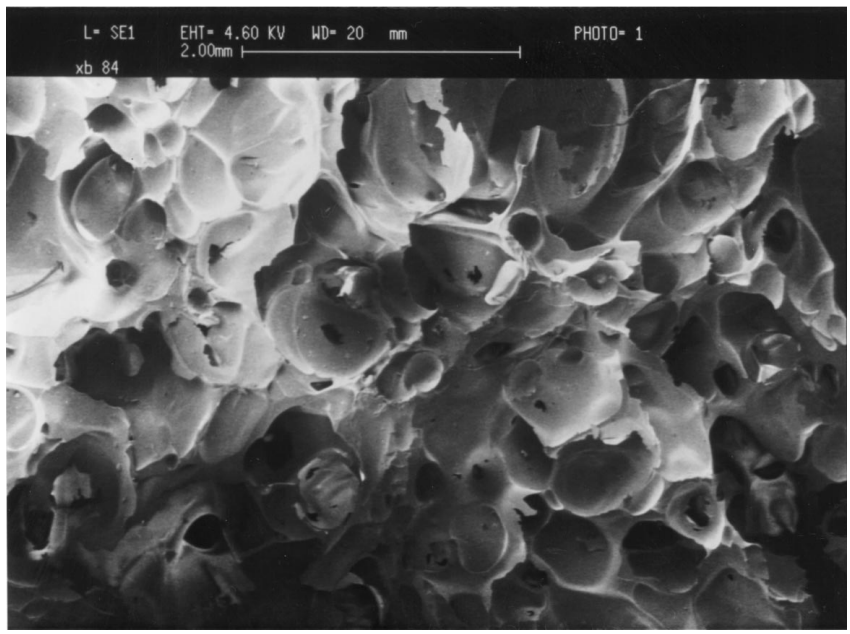

(a)

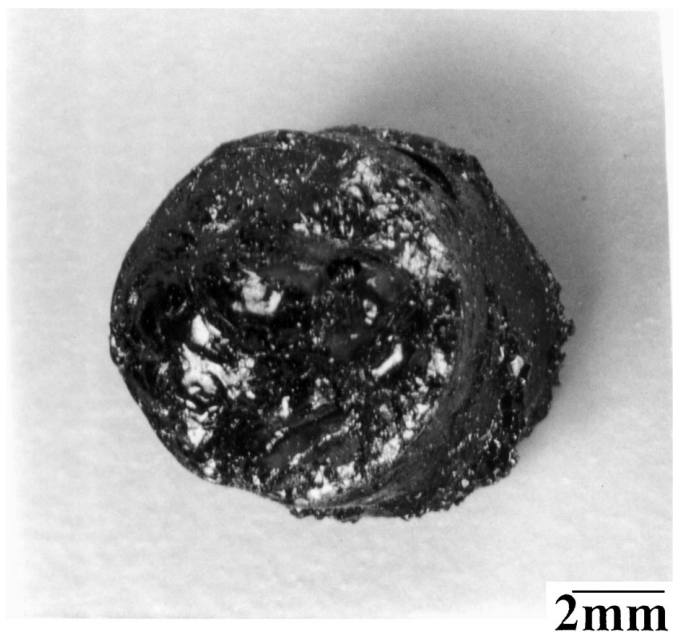

(b)

Figure 6 (a) Scanning electron micrograph of cross-section and (b) macro-appearance of pyrolyzed polymeric precursor P5.

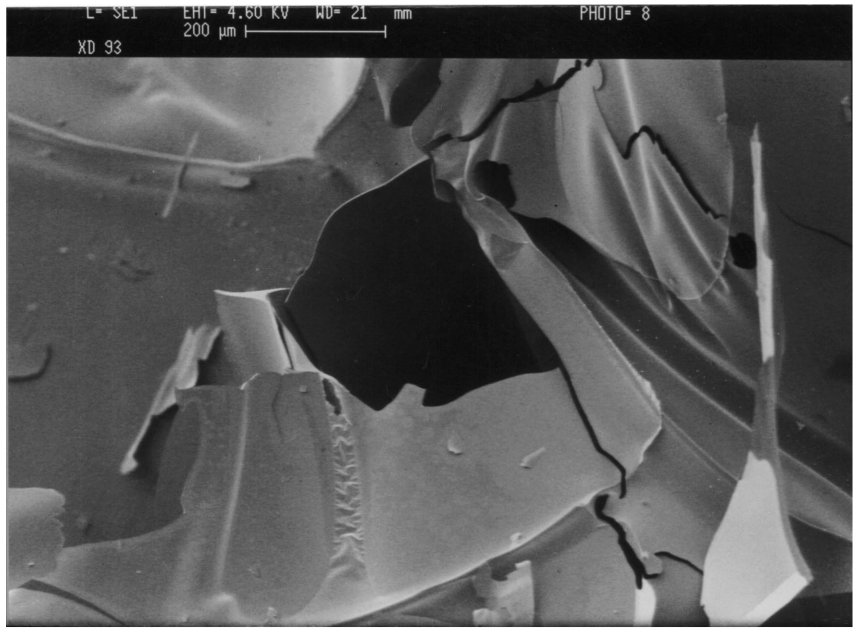

(a)

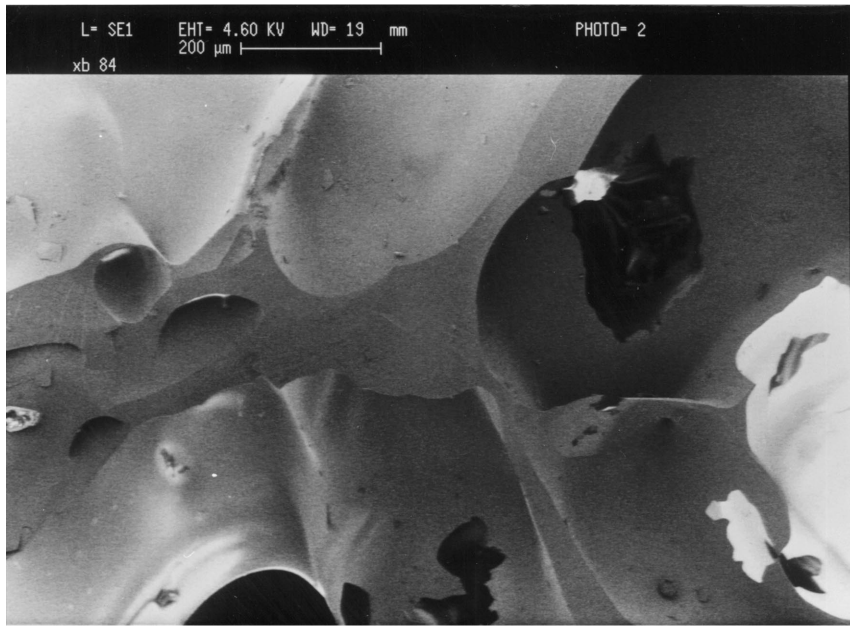

(b)

Figure 7 Scanning electron micrograph of cross-section of pyrolyzed polymeric precursor (a) P2 and (b) P5 showing regions adjacent to the pores.

3.2. Conversion to ceramic

The XRD patterns of the residues heated to over 1100 °C showed that the polysilanes synthesized produced SiC on pyrolysis. Taking P5 as an example, XRD results (Fig. 2) suggest that the residues obtained after heating in nitrogen were amorphous up to 1100 °C, and then gradually crystallized as the temperature was increased. Three characteristic peaks were observed in the crystallized materials at $2\theta = 36, 61$, and 72°, which correspond to the (111), (220), and (311) planes of β-SiC, respectively [29, 30].

The thermogravimetric traces of the polysilanes are shown in Fig. 3 and the final pyrolytic yield of each polymer is given in Table II. It is apparent that the SiC yield is very dependent on the composition of the polymers. Co- and ter-polymers give better SiC yields, compared with the homopolymer P1. This can be attributed to the crosslinked structures formed during the pyrolysis due to the thermal cross-linking capability of hydrosilane (Si-H) and vinyl (CH_2=CH) groups in the polymeric precursors and the branched structures generated during polymerization due to the addition of trichloromethylsilane or trichlorophenylsilane monomers [14–16, 27–30].

3.3. Formation of SiC foam

It is generally believed that pore formation in the ceramics derived from polymeric precursors is due to dissociation reactions which occur during pyrolysis of the

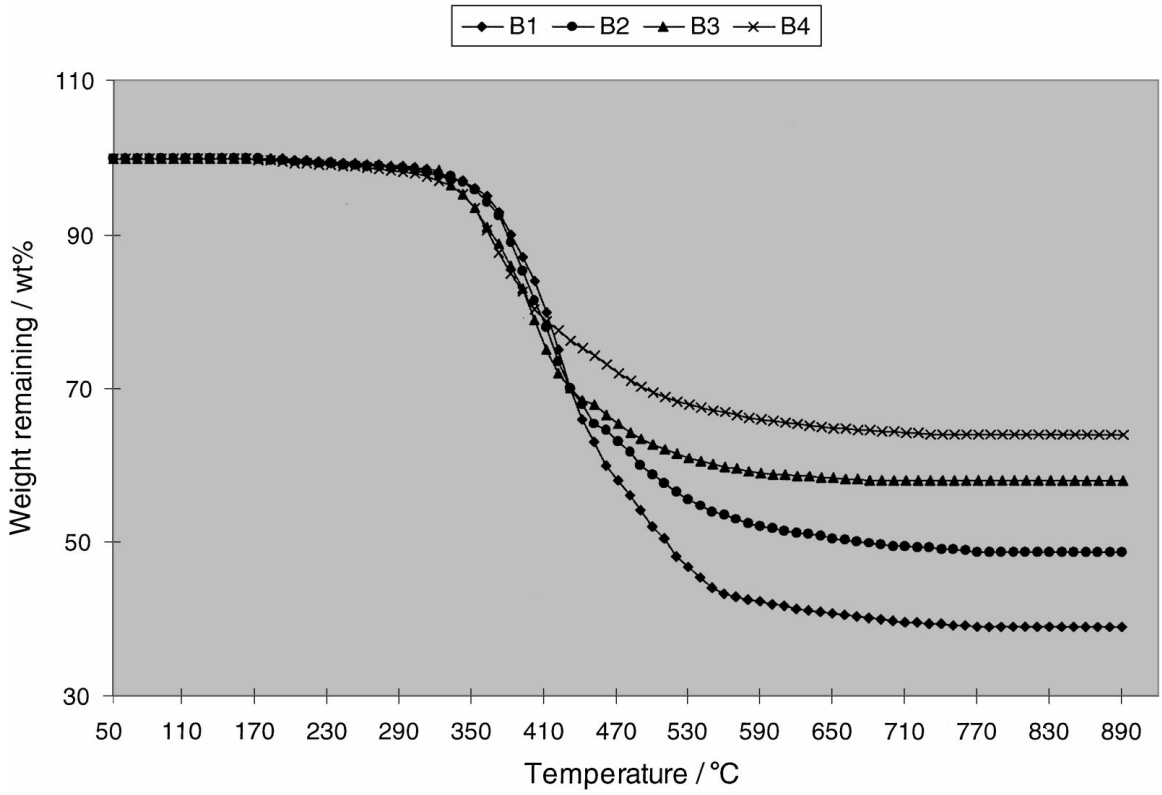

Figure 8 Thermogravimetric traces of polymer blends B1–B4.

polymers where small molecules such as hydrogen and methane are formed and initially exist in the dissolved state. When the preceramic polymer becomes supersaturated with the volatiles, nucleation and formation of gas bubbles occur. The process of conversion from a polymer to ceramic restrains and eventually arrests the growth of such bubbles which ultimately become pores in the final ceramic product [31, 32].

As shown in the Fig. 3, the pyrolysis process of the polymers may be considered to takes place in three consecutive stages. In the first stage (up to 300 °C), a very slow rate of weight loss (total of less than 2%) occurs and this is characteristic of high molecular weight polymers. In the second stage (300–700 °C), a major weight loss takes place, due to the decomposition and re-arrangement of the polymers and small molecules consisting mainly of methane and hydrogen are evolved [28]. In the third and final stage of pyrolysis (above 700 °C), a further weight loss of ca. 2% occurs as the samples are heated to 900 °C. Pore formation occurs predominantly during the second stage of pyrolysis [31, 32].

Macro-photographs and scanning electron micrographs of the pyrolyzed polysilanes (Figs 4, 5 and 6) indicate that there is a relationship between the polymer structure and porosity of the ceramic produced. In general, the pore sizes of the ceramics decreased with the increase of the functionality and pyrolytic yield of the polymeric precursor. The precursors with lower functionality (e.g. P1 and P2 in the Table II) gave lower pyrolytic yields and the post-pyrolysis pore size ranged from 700–1800 μm. Some pores were covered by thin membranes, i.e. a partially open pore structure was formed (Fig. 4a). These ceramic foams lost their original disc shapes during pyrolysis because of melting of the polymer as temperature increased (Fig. 4b). On the other hand, the precursors with higher functionality (e.g. P8, and P9 in Table II) gave higher pyrolytic yields and produced a more densified ceramic with fine pores in the size range 5–20 μm (Fig. 5a). These ceramics maintained their original shape very well (Fig. 5b). Actually, after pyrolysis these polysilane precursors formed micro-porous ceramics rather than ceramic foams. In the present work, the best ceramic foams were obtained by pyrolyzing polymeric precursors with intermediate functionalities and pyrolytic yields. These also produced a partially open pore-structure but with a more uniform pore distribution and a smaller pore size range of 400–800 μm (Fig. 6a). These discs also retained their original shape reasonably well during pyrolysis (Fig. 6b).

It is noteworthy that the ceramic foams derived from polysilanes with lower pyrolytic yields showed cracks adjacent to the pores (Fig. 7a). Such defects were largely absent in the foams produced from polysilanes with intermediate pyrolytic yields (Fig. 7b). It was also observed that in all cases the pores were distributed throughout the cross-section without an apparent pattern, although a better pore distribution was obtained in the ceramic foams produced from precursors which gave intermediate pyrolytic yields. This is probably because these foams were produced by using surface heating in a furnace and here the heating rate is non-uniform in the interior of these samples. A more uniform size distribution of the pores can be obtained by using microwave heating.

Another strategy used in this study to control pore formation in the ceramic foams is the mixing of

TABLE III Details of the blends and their final pyrolytic yields

Blends	P2/P9 ratio (wt %)	Pyrolytic yield (wt %)
B1	80/20	38.9
B2	60/40	48.9
B3	40/60	59.0
B4	20/80	64.1

different polymeric precursors to produce polymer blends which are pyrolyzed subsequently. Therefore, a polymeric precursor (P2) with a low pyrolytic yield and the another with a high pyrolytic yield (P9) were chosen to make polymer blends. The compositions of the blends and their final pyrolytic yields are given in Table III. The blends showed similar thermogravimetric traces (Fig. 8) to those of the individual polymers (Fig. 3), where the pyrolysis process occurs in three stages and the major weight loss takes place from 300 to 700 °C. However, it can be seen that the final pyrolytic yields of the blends can be controlled systematically by varying the weight ratios of the polymers used (Fig. 8). This also results in different pore morphologies as shown in Figs 9 and 10. As in the case of the single precursors, the pore size of the SiC produced from the polymer blends decreased with the increase of the pyrolytic yield. The blend which gave the lowest pyrolytic yield (B1) contained large open pores (Fig. 9a) and lost its original disc shape during pyrolysis (Fig. 9b). In contrast, the blend which gave the highest pyrolytic yield (B4) mostly contained fine pores (Fig. 10a) and

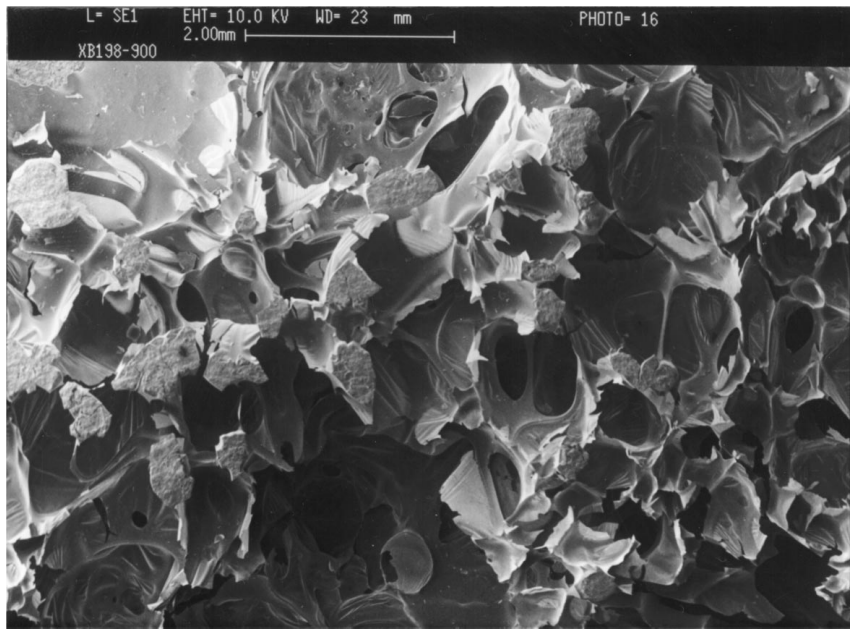

(a)

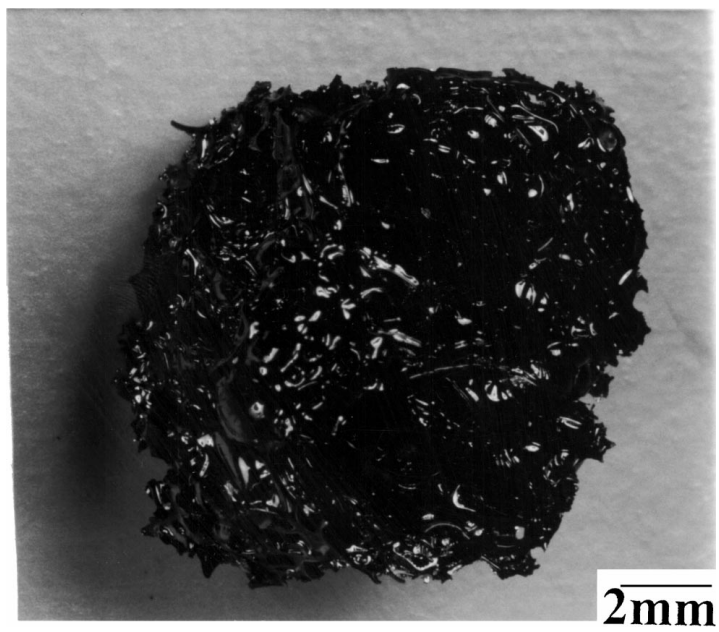

(b)

Figure 9 (a) Scanning electron micrograph of cross-section and (b) macro-appearance of pyrolyzed polymeric precursor B1.

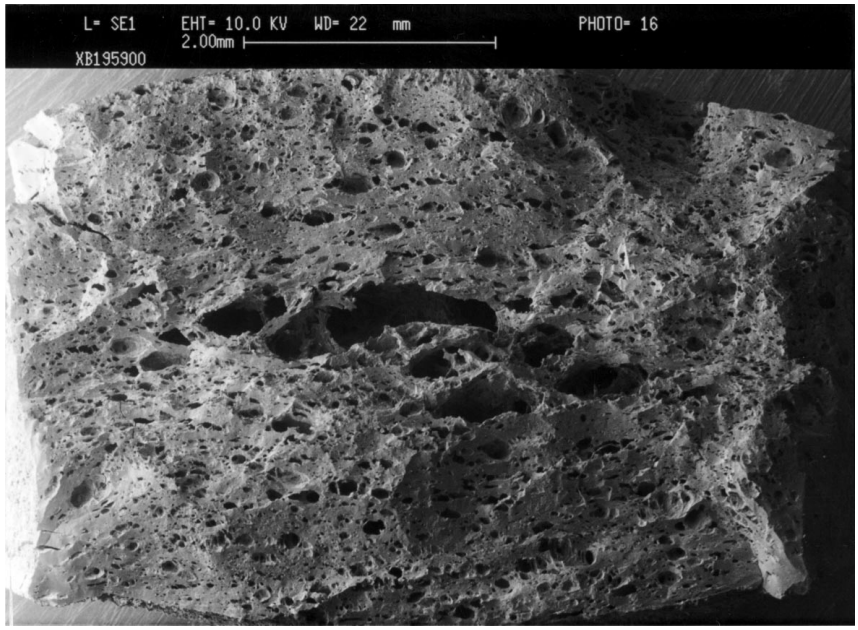

(a)

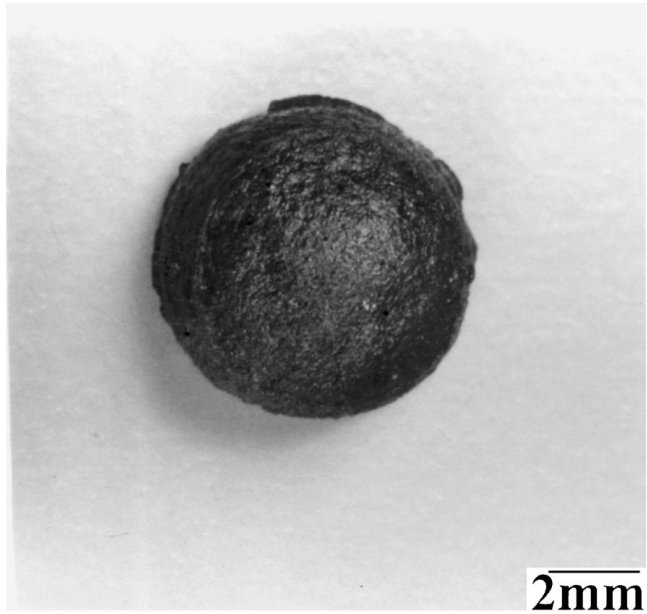

(b)

Figure 10 (a) Scanning electron micrograph of cross-section and (b) macro-appearance of pyrolyzed polymeric precursor B4.

retained its original shape very well (Fig. 10b). Blends B2 and B3 which are in between formulations B1 and B4 (Table III) showed intermediate characteristics. The synthesis of ceramic foams from polymeric precursor blends therefore offers a more controllable procedure where the pyrolytic yield can be adjusted to suite leading to pre-determined levels of the porosity and pore features.

4. Conclusions

Methodology for producing SiC foams from preceramic polymers has been demonstrated by using polysilanes and their blends as precursors. It was found that features of the ceramic foams produced were dependent on the compositions and the structures of the precursors pyrolyzed. The polymers with higher functionalities gave higher pyrolytic yields due to cross-linking or branched structures formed during polymerization and pyrolysis and the corresponding ceramics produced had micropores and shape retention was good. On the other hand, polymers with lower functionalities gave lower pyrolytic yields and ceramics with partially open-pore structures but shape retention during pyrolysis was poor. In the present work, the best SiC foams were produced using polysilane precursors with pyrolytic yields between 50–60 wt %. These foams retained their original shapes reasonably well. Polymer blends of two different precursors could be more effectively used to control the final pyrolytic yield, shape-retainability and the porosity of the ceramics produced by varying the proportions of the precursors in the blends.

Acknowledgements

The authors wish to thank the Government of Pakistan for partial support of this work via a PhD scholarship to Mr. Nangrejo. Mr. F. Page is thanked for help in electron microscopy. The support of Mr. T. J. Atkinson in resolving technical matters is acknowledged.

References

1. R. W. RICE, "Porosity of Ceramics" (Marcel Dekker Inc., 1998).
2. J. SAGGIO-WOYANSKY, C. E. SCOTT and W. P. MINNEAR, *Amer. Ceram. Soc. Bull.* **71** (1992) 1674.
3. E. J. A. E. WILLIAMS and J. R. G. EVANS, *J. Mater. Sci.* **31** (1996) 559.
4. F. F. LANGE and K. T. MILLER, *Adv. Ceram. Mater.* **2** (1987) 827.
5. S. B. BHADURI and Z. B. QIAN, *J. Mater. Synth. Proc.* **3** (1995) 361.
6. A. J. SHERMAN, R. H. TUFFIAS and R. B. KAPLAN, *Amer. Ceram. Soc. Bull.* **70** (1990) 1025.
7. M. WU and G. L. MESSING, *J. Amer. Ceram. Soc.* **73** (1990) 3497.
8. Y. AOKI and B. McENANEY, *Brit. Ceram. Trans.* **94** (1995) 133.
9. P. SEPULVEDA, *Amer. Ceram. Soc. Bull.* **76** (1997) 61.
10. R. W. PEKALA and R. W. HOPPER, *J. Mater. Sci.* **22** (1987) 1840.
11. J. D. LEMAY, R. W. HOPPER, L. W. HRUBESH and R. W. PEKALA, *Mater. Res. Soc. Bull.* **15** (1990) 19.
12. T. J. FITZGERALD and A. MORTENSEN, *J. Mater. Sci.* **30** (1995) 1025.
13. P. COLOMBO and M. MODESTI, in Proc. of 9th CIMTEC, Florence, Italy, 1998.
14. S. YAJIMA, J. HAYASHI, K. OKAMURA and M. OMORI, *J. Amer. Ceram. Soc.* **59** (1976) 324.
15. R. WEST, L. DAVID, P. I. DJUROVICH, H. YU and R. SINCLAIR, *Amer. Ceram. Soc. Bull.* **62** (1983) 899.
16. C. L. SCHILLING, *Brit. Polym. J.* **18** (1986) 355.
17. D. SEYFERTH, G. E. KOPPETSCH, T. G. WOOD, H. J. TRACY, J. L. ROBISON, P. CZUBAROW, M. TASI and H.-G. WOO, *Polym. Prepr. (Amer. Chem. Soc., Div. Polym. Chem.)* **34**(1) (1993) 223.
18. W. R. I. CRANSTONE, S. M. BUSHNELL-WATSON and J. H. SHARP, *J. Mater. Res.* **10** (1995) 2659.
19. A. T. HEMIDA, M. BIROT, J. P.PILLOT, J. DUNOGUES and R. PAILLER, *J. Mater. Sci.* **32** (1997) 3475.
20. P. GREIL, *J. Amer. Ceram. Soc.* **78** (1995) 835.
21. X. BAO, M. J. EDIRISINGHE, G. F. FERNANDO and M. J. FOLKES, *J. Euro. Ceram. Soc.* **18** (1998) 915.
22. *Idem., Brit. Ceram. Trans.* **97** (1998) 253.
23. X. BAO and M. J. EDIRISINGHE, *J. Mater. Sci. Lett.* **17** (1998) 1644.
24. J. P. WESSON and T. C. WILLIAMS, *J. Polym. Sci. Polym. Chem.* **17** (1979) 2833.
25. *Idem., ibid.* **18** (1980) 959.
26. *Idem., ibid.* **19** (1981) 65.
27. D. J. CARLSSON, J. D. COONEY, S. GAUTHIER and D. J. WORSFOLD, *J. Amer. Ceram. Soc.* **73** (1990) 237.
28. F. I. HURWITZ, T. A. KACIK, X.-Y. BU, J. MASNOVI, P. J. HEIMANN and K. BEYENE, *J. Mater. Sci.* **30** (1995) 3130.
29. W. R. SCHMIDT, L. V. INTERRANT, R. H. DOREMUS, T. K. TROUT, P. S. MARCHETTI and G. E. MACIEL, *Chem. Mater.* **3** (1991) 257.
30. Y.-T. SHIEH and S. P. SAWAN, *J. Appl. Polym. Sci.* **58** (1995) 2013.
31. M. BLANDER and J.L. KATZ, *AIChE J.* **21** (1975) 833.
32. H. YAO, S. KOVENKLIOGLU and D. M. KALYON, *Chem. Eng. Comm.* **96** (1990) 155.

Received 3 November
and accepted 18 November 1998